

The Standard Model in Strong Fields: Electroweak Radiative Corrections for Highly Charged Ions.

Ilya Bednyakov, Leonti Labzowsky

*Institute of Physics, St.Petersburg State University, 198904 Uljanovskaya 1, Petrodvorets,
St.Petersburg, Russia*

Günter Plunien, Gerhard Soff

*Institut für Theoretische Physik, Technische Universität Dresden, Mommsenstrasse 13, D-01062
Dresden, Germany*

Valentin Karasiev

Instituto Venezolano de Investigaciones Cientificas Caracas, Venezuela

(November 13, 2018)

Abstract

Electroweak radiative corrections to the matrix elements $\langle ns_{1/2} | \hat{H}_{\text{PNC}} | n'p_{1/2} \rangle$ are calculated for highly charged hydrogenlike ions. These matrix elements constitute the basis for the description of the most parity nonconserving (PNC) processes in atomic physics. The operator \hat{H}_{PNC} represents the parity nonconserving relativistic effective atomic Hamiltonian at the tree level. The deviation of these calculations from the calculations valid for the momentum transfer $q^2 = 0$ demonstrates the effect of the strong field, characterized by the momentum transfer $q^2 = m_e^2$ (m_e is the electron mass). This allows for a test of the Standard Model in the presence of strong fields in experiments with highly charged ions.

I. INTRODUCTION

PNC experiments in atomic physics provide an important possibility to deduce informations on the Standard Model independent of high-energy physics experiments. The recent LEP experiments [1], that yield extremely accurate values for Z-boson properties, correspond to the resonant process. This means that all the nonresonant corrections are strongly suppressed. Hence this might not be the most convincing way for the search of all types of “new physics” beyond the minimal Standard Model, e.g., for the existence of a second Z-boson etc.

The observation of “new physics“ in atomic physics experiments is most probable related to processes beyond the tree level, for which electroweak radiative corrections are taken into account. This question was thoroughly discussed by many authors, in particular in [2] - [6]. Atomic PNC experiments are usually performed with heavy atoms (Cs, Tl, Pb, Bi) due to the strong enhancement of PNC effects with increasing nuclear charge number Z , which was first noticed by Bouchiat and Bouchiat [7]. However, the electrons involved in various PNC processes in these atoms are loosely bound valence electrons and the corresponding momentum transfer is much smaller than the squared rest mass of the electron:

$$q^2 \ll m_e^2 . \tag{1}$$

The situation is different in highly charged ions (HCI), where $q^2 \approx m_e^2$. This peculiar property of HCI was a reason for many experimental and theoretical efforts to “test” QED in strong fields. In particular experimental [8] - [11] and theoretical [12] - [17] attempts were made recently to verify the Lamb shift in one-electron heavy ions up to the second order in the fine structure constant α . These attempts are yet uncomplete from both sides. Therefore there would be even a deeper reason to test the validity of the Standard Model in strong fields. We should emphasize here that the concept of the strong field is not constrained to the large momentum transfer in some particular processes. The latter often occurs in high energy physics collision experiments. During the collision period the particles

are also influenced by the strong field. However, for the tightly bound electron in HCl this strong field is present for a relatively long time, defined by the lifetime of the corresponding electronic state.

In this paper we show that the test of the Standard Model (or the search for “new physics” beyond the Standard Model) is possible in experiments with HCl. Thus PNC experiments in HCl can open a new field of research independent of the successes of PNC experiments in neutral atoms.

We calculate electroweak radiative corrections to the matrix element $F_0 = \langle ns_{1/2} | \hat{H}_{\text{PNC}} | n'p_{1/2} \rangle$, which represents the basis for most parity nonconserving processes studied in atomic physics of highly charged ions. Here the operator \hat{H}_{PNC} indicates the parity nonconserving relativistic effective atomic Hamiltonian at the tree level. The electroweak radiative corrections will be provided by $\langle ns_{1/2} | \hat{H}_{\text{PNC}}^{\text{rad}} | n'p_{1/2} \rangle \equiv F_{\text{SF}}^{\text{rad}}$.

Previously radiative electroweak corrections were calculated for the case of low momentum transfer ($q^2 = 0$) or for the low field case, that is valid for neutral atoms. We are following the work by Lynn and Sandars [6] who represented their results in the factorized form

$$\hat{H}_{\text{PNC}}^{\text{rad}} = \delta A_{\text{PNC}}^{\text{rad}} \hat{H}_{\text{PNC}} \quad (2)$$

where the factor $\delta A_{\text{PNC}}^{\text{rad}}$ is independent of electron variables. This factorization is possible only in the low field case. Thus the quantity corresponding to $F_{\text{SF}}^{\text{rad}}$ in the low field case should be defined as

$$F_{\text{LF}}^{\text{rad}} = \delta A_{\text{PNC}}^{\text{rad}} \langle ns_{1/2} | \hat{H}_{\text{PNC}} | n'p_{1/2} \rangle . \quad (3)$$

The deviation of the function $f^{\text{rad}} \equiv \frac{F_{\text{SF}}^{\text{rad}}(Z) - F_0(Z)}{F_{\text{LF}}^{\text{rad}}(Z) - F_0(Z)}$ from unity for large Z values will manifest the existence of strong field effects for electroweak radiative corrections in the Standard Model.

The electroweak radiative corrections to the matrix element $\langle ns_{1/2} | \hat{H}_{\text{PNC}} | n'p_{1/2} \rangle$ can be partitioned into the corrections $\langle ns_{1/2} | \hat{H}_{\text{PNC}}^{\text{rad}} | n'p_{1/2} \rangle$ to the PNC operator and to corrections to the wave functions. The corrections to the wave functions were not considered in [6].

Moreover, the full treatment requires the evaluation of radiative corrections to the total expression of the PNC atomic amplitude, including the PNC matrix element and the photon emission(absorption) matrix element. In this paper we will concentrate on radiative corrections to the PNC matrix element.

In section 2 of this paper we analyse the influence of strong fields on different electroweak corrections. In section 3 we evaluate electroweak radiative loop corrections to the PNC operator. In section 4 the loop corrections to wave functions are evaluated. Section 5 contains the discussion of the numerical results and conclusions.

II. ANALYSIS OF ELECTROWEAK RADIATIVE CORRECTIONS IN HIGHLY CHARGED IONS

In this paper we will consider only the nuclear spin-independent part of \hat{H}_{PNC} :

$$\hat{H}_{\text{PNC}} = A_{\text{PNC}} \gamma_5 \rho_N(r) , \quad (4)$$

where γ_5 is the Dirac matrix and $\rho_N(r)$ is the nuclear density. In the original Bouchiat formulation [7] the constant A_{PNC} reads

$$A_{\text{PNC}} = \frac{G_F Q_W}{2\sqrt{2}} , \quad (5)$$

where G_F is the Fermi constant and Q_W is the “weak charge” of the nucleus. At the tree level Q_W is given by

$$Q_W = -N + Z(1 - 4s^2) , \quad (6)$$

where $s^2 = \sin^2 \theta_W$, θ_W is the Weinberg angle, N is the number of neutrons in the nucleus.

In the following we will also utilize the equivalent Sandars definition of A_{PNC} [18]:

$$A_{\text{PNC}} = \frac{\pi\alpha}{4M_Z^2} P_W , \quad (7)$$

where α is the fine structure constant and M_Z is the mass of Z-boson. At the tree level we have

$$P_W = \frac{-N + Z(1 - 4s^2)}{s^2(1 - s^2)}. \quad (8)$$

According to Lynn and Sandars [6], all the electroweak radiative corrections can be divided in two classes. The first class, called “oblique” corrections, corresponds to the Feynman graphs depicted in Fig. 1. These corrections can be incorporated into the running coupling constants, dependent on q^2 . To include the “oblique” corrections into the PNC calculations for neutral atoms, Lynn and Sandars employ the running fine structure constant $\alpha^*(q^2 = 0)$, the sine of the Weinberg angle $s^*(q^2 = 0)$ and the mass of the Z-boson $M_Z^2(q^2 = 0)$. The Fermi constant G_F does not enter the Sandars description of PNC effects. In the case of atomic experiments $\alpha^*(q^2 = 0) = \alpha$, where α is the standard atomic value, s and M_Z^* are obtained from the LEP values [1] by scaling to $q^2 = 0$.

The remarkable feature of Sandars description is that for all heavy elements of experimental interest P_W is very close to $-\frac{16}{3}N$ and is weakly dependent on s^2 [18]. Therefore it is convenient to introduce the quantity

$$\tilde{P}_W = -\frac{3}{16N}P_W. \quad (9)$$

Then the “oblique” radiative corrections can be included in \tilde{P}_W

$$\tilde{P}_W = \tilde{P}_W^* (1 + \delta_P^M), \quad (10)$$

where \tilde{P}_W^* is defined from Eq. (8) with $s^2 = s^{*2}(q^2 = 0) = 0.2394$. The correction δ_P^M results as [6]

$$\delta_P^M = \frac{M_Z^2}{[M_Z^*(q^2 = 0)]^2} - 1 \simeq 0.0880. \quad (11)$$

Returning to our problem for HCl, we emphasize that we are interested to follow the change of the running constants in the interval from $q^2 = 0$ to $q^2 = m_e^2 = (0.5 \text{ MeV})^2$. This interval is 10^5 times smaller than the interval from $q^2 = 0$ to $q^2 = M_Z^2 = (91 \text{ GeV})^2$. Therefore the value δ_P^M should be considered as field independent. Our goal is to search for the field dependent radiative corrections and to compare them with the value given by Eq. (11). In

section 3 of this paper we will evaluate loop corrections directly, using the extension of the Furry picture of QED for tightly bound electrons. In the Furry picture the electrons are considered from the beginning in the external field of the nucleus. The Feynman rules for QED in the Furry picture can be found, for example, in [19].

To represent the basic atomic PNC matrix element in the Furry picture we have to consider first the Feynman graph corresponding to the exchange of a Z-boson between the atomic electron and the quark. Due to the vector current conservation the Z-boson coupling to the quarks in the case of an atom transforms to the Z-boson coupling to nucleons and to the nucleus. Thus the quark line in the Feynman graph should be replaced by the nuclear line. Moreover, the interaction of the electron with the nucleus via the exchange of a Z-boson can be replaced by the interaction with the electroweak external field described by Eq. (4). This corresponds to the Feynman graph depicted in Fig. 2.

Now we can draw the Feynman graphs corresponding to loop corrections in the Furry picture of the Standard Model for tightly bound electrons. We suppose that the main contribution to the difference between the cases of $q^2 = m_e^2$ (HCI) and $q^2 = 0$ (neutral atoms) arises from electron loops, since the heavier particle loops should be less sensitive to the strong field effect. In this respect we have to consider the graphs presented in Fig. 3 a)-d). In the evaluation of these graphs we utilize the Uehling approximation. Then the bound electron loop is approximated by the first term of the expansion in powers of the external potential (cf. Fig. 4 a)-d)). The Uehling approximation is justified even for tightly bound electrons in QED. The evaluation of electron loop corrections corresponding to Fig. 4 a), b) will be performed in section 3. In section 4 we will investigate the corrections corresponding to Fig. 4 c), d), i.e. the corrections to the wave functions.

The other type of electroweak radiative corrections, called “specific” [6], corresponds to Feynman graphs displayed in Figs. 5 and 6. Fig. 5 represents the contribution of the electron weak anapole moment, Fig. 6 corresponds to the vertices that describe the electromagnetic renormalization of the Z-boson coupling. According to our analysis only these

graphs can contribute to the difference between the strong field and low field cases.

Lynn and Sandars [6] present the electroweak radiative corrections to \tilde{P}_W in the form:

$$\tilde{P}_W = \tilde{P}_W^*(1 + \delta_P^M) + \delta_P^{\text{anapole}} + \delta_P^{\text{vertex}} \quad (12)$$

where \tilde{P}_W^* and δ_P^M are defined by Eqs. (10) and (11), δ_P are specific radiative corrections to \tilde{P}_W . In Eq. (12) we omitted small field-independent "specific" corrections given by the "box" Feynman graphs [6].

We present the results of our calculations in the form

$$\Delta_{\text{rad}} = \Delta\tilde{P}_W + \delta_P^{\text{w.f.}} \quad (13)$$

with

$$\begin{aligned} \Delta\tilde{P}_W = & \delta_P^{\text{loop-op}}(f_{\text{loop-op}}^{\text{rad}} - 1) \\ & + \delta_P^{\text{anapole}}(f_{\text{anapole}}^{\text{rad}} - 1) + \delta_P^{\text{vertex}}(f_{\text{vertex}}^{\text{rad}} - 1), \end{aligned} \quad (14)$$

where $\Delta\tilde{P}_W$ is the difference between the corrections for HCI and neutral atoms, $\delta_P^{\text{loop-op}}$, $\delta_P^{\text{anapole}}$ and δ_P^{vertex} denote the $q^2 = 0$ limit for the different radiative corrections to the PNC operator, and the functions f^{rad} are defined in the Introduction. Actually in this paper only the term $\delta_P^{\text{loop-w.f.}}$, the most important after δ_P^M , will be calculated numerically. This term represents the loop corrections to the wave functions.

III. LOOP CORRECTIONS TO THE PNC OPERATOR

We begin with the evaluation of the corrections of Fig. 4 a). To write down the corresponding matrix element we use the standard Feynman rules formulated for the QED of tightly bound electrons [19]. These rules are easily extended to the Standard Model calculations. The S-matrix element corresponding to the Feynman graph of Fig. 4 a) is given by

$$\begin{aligned} S = & (-i)^2 g^2 \int d^4x_1 d^4x_2 d^4x_3 \bar{\psi}_{ns_{1/2}}(x_1) \gamma^\mu (\gamma_5 - \eta) \psi_{n'p_{1/2}}(x_1) \\ & \times D_{\mu\nu}^Z(x_1 - x_2) \text{Tr}[\gamma^\nu (\gamma_5 - \eta) S^0(x_2 - x_3) \gamma^\lambda S^0(x_3 - x_2)] A_\lambda^{\text{ext}}(x_3), \end{aligned} \quad (15)$$

where $\eta = 1 - 4 \sin^2 \theta_W$, Tr corresponds to the Dirac matrices, that enter the electron loop. The Z-boson propagator $D_{\mu\nu}^Z$ in momentum space can be expressed as

$$D_{\mu\nu}^Z(k) = -\frac{4\pi i g_{\mu\nu}}{k^2 - M_Z^2 + i0}. \quad (16)$$

We will use the expression for $D_{\mu\nu}^Z(x_1 - x_2)$ in coordinate space

$$D_{\mu\nu}^Z(x_1 - x_2) = \int \frac{d\omega}{2\pi} e^{-i\omega(t_1 - t_2)} D_{\mu\nu}^Z(\vec{x}_1 - \vec{x}_2, \omega) \quad (17)$$

where

$$D_{\mu\nu}^Z(\vec{x}_1 - \vec{x}_2, \omega) = -i4\pi g_{\mu\nu} \int \frac{d^3k}{2\pi} \frac{e^{i\vec{k} \cdot (\vec{x}_1 - \vec{x}_2)}}{\omega^2 - \vec{k}^2 - M_Z^2 + i0}. \quad (18)$$

The external electromagnetic field $A_\nu^{\text{ext}}(x)$ reads

$$A_\nu^{\text{ext}}(x) = \delta_{\nu 0} eU(\vec{x}) \quad (19)$$

where $U(\vec{x})$ is the electric field of the nucleus (point-like or extended). $S^0(x - y)$ is the free electron propagator

$$S^0(x - y) = \frac{1}{(2\pi)^4} \int d^4p S^0(p) e^{-ip(x-y)} \quad (20)$$

with

$$S^0(p) = i \frac{\not{p} + m_e}{p^2 - m_e^2}. \quad (21)$$

The wave functions $\bar{\psi}_{ns_{1/2}}, \psi_{n'p_{1/2}}$ are the eigenvectors of the Dirac equation for the electron in the field of the nucleus

$$\psi_n(x) = e^{-iE_n t} \psi_n(\vec{x}), \quad (22)$$

where E_n are the corresponding Dirac eigenvalues. The Standard Model constant g is equal to

$$g^2 = \frac{e^2}{s^2}, \quad (23)$$

where e is the electron charge. We employ the pseudoeuclidean metric with the usual metric tensor $g_{\mu\nu}$. γ_μ, γ_5 are the usual Dirac matrices.

The S -matrix element is connected with the amplitude by the relation

$$S_{if} = 2\pi i \delta(E_i - E_f) M_{if} \quad (24)$$

where M_{if} is the amplitude and E_i, E_f are the initial and final state energies of the system. Transforming to the momentum space in expression (15) and integrating over the frequency variables, we obtain

$$M_{if} = -\frac{(1-4s^2)}{16c^2s^2} \frac{1}{8\pi^2} \int d^3p_1 d^3p_2 \bar{\psi}_{ns_{1/2}}(\vec{p}_1) \frac{eU(\vec{q})}{\vec{q}^2 + M_Z^2} \gamma_0 \gamma_5 \Pi(0, \vec{q}^2) \psi_{n'p_{1/2}}(\vec{p}_2) \quad (25)$$

where $\vec{q} = \vec{p}_1 - \vec{p}_2$. In the expression (25) we retain only the parity violation terms. These terms contain the γ_5 matrix in one of the vertices connected with Z-boson. The vertex connected with the loop yields a zero result due to the identities:

$$\text{Tr}(\gamma_\mu \gamma_\nu \gamma_5) = 0, \quad (26)$$

$$\text{Tr}(\gamma_\mu \gamma_\nu \gamma_\alpha \gamma_\beta \gamma_5) = i\epsilon_{\mu\nu\alpha\beta}, \quad (27)$$

where $\epsilon_{\mu\nu\alpha\beta}$ is the unit antisymmetrical tensor. This tensor appears in the combination with the symmetrical product $p_\mu p_\nu$, so that

$$\epsilon_{\mu\nu\alpha\beta} p_\mu p_\nu = 0. \quad (28)$$

The function $\Pi(\vec{q}^2)$ is divergent and should be renormalized. We shall use from the very beginning the known renormalized expression $\Pi_R(q^2)$ (cf. for example [20])

$$\Pi_R(q^2) = \frac{2ie^2}{2\pi^2} q^2 \int_0^1 dx x(1-x) \ln \left[1 - \frac{q^2}{m_e^2} x(1-x) \right]. \quad (29)$$

Since all the integrations in Eq. (25) after the insertion of the renormalized expression (29) are convergent, we can omit \vec{q}^2 in the denominator. In the case of the pure Coulomb potential with

$$U(\vec{q}) = 4\pi \frac{eZ}{\vec{q}^2} \quad (30)$$

we obtain

$$M_{if} = \frac{(1-4s^2)}{2c^2s^2} \frac{e^3Z}{(2\pi)^2} \frac{1}{M_Z^2} \int_0^1 dx x(1-x) \int d^3p_1 d^3p_2 \bar{\psi}_{ns_{1/2}}(\vec{p}_1) \gamma_0 \gamma_5 \ln \left[1 + \frac{\vec{q}^2}{m_e^2} x(1-x) \right] \psi_{n'p_{1/2}}(\vec{p}_2). \quad (31)$$

We consider first the low field limit of Eq. (31). Then $\vec{q}^2/m_e^2 \ll 1$ and we can write

$$M_{if} = -\frac{(1-4s^2)}{16c^2s^2} \frac{e^2Z}{\pi^3} \frac{e^2}{m_e^2 M_Z^2} \int_0^1 dx x^2(1-x)^2 \times \left[\int d^3p_1 d^3p_2 \varphi_{ns_{1/2}}^+(\vec{p}_1) \vec{q}^2 \chi_{n'p_{1/2}}(\vec{p}_2) + \int d^3p_1 d^3p_2 \chi_{ns_{1/2}}^+(\vec{p}_1) \vec{q}^2 \varphi_{n'p_{1/2}}(\vec{p}_2) \right], \quad (32)$$

where φ, χ are the upper and lower components of the Dirac wave function, respectively.

Transforming to the coordinate representation we obtain

$$M_{if} = \frac{(1-4s^2)}{16c^2s^2} \frac{e^2Z}{\pi^3} \frac{e^2(2\pi)^3}{m_e^2 M_Z^2} \int_0^1 dx x^2(1-x)^2 \times \left[\int d^3r_1 d^3r_2 \varphi_{ns_{1/2}}^+(\vec{r}_1) (\vec{\nabla}_1 + \vec{\nabla}_2)^2 \delta(\vec{r}_1) \delta(\vec{r}_2) \chi_{n'p_{1/2}}(\vec{r}_2) + \int d^3r_1 d^3r_2 \chi_{ns_{1/2}}^+(\vec{r}_1) (\vec{\nabla}_1 + \vec{\nabla}_2)^2 \delta(\vec{r}_1) \delta(\vec{r}_2) \varphi_{n'p_{1/2}}(\vec{r}_2) \right]. \quad (33)$$

Finally we find:

$$M_{if} = \frac{1-4s^2}{12c^2s^2} \frac{e^4Z}{\pi} \frac{\pi}{m^2 M_Z^2} \int_0^1 dx x^2(1-x)^2 \left[\nabla^2 \varphi_{ns_{1/2}}^+(0) \chi_{n'p_{1/2}}(0) + \varphi_{ns_{1/2}}^+(0) \nabla^2 \chi_{n'p_{1/2}}(0) + 2\vec{\nabla} \varphi_{ns_{1/2}}^+(0) \cdot \vec{\nabla} \chi_{n'p_{1/2}}(0) + \chi_{n'p_{1/2}}^+(0) \nabla^2 \varphi_{n'p_{1/2}}(0) + 2\vec{\nabla} \chi_{n'p_{1/2}}^+(0) \cdot \vec{\nabla} \varphi_{n'p_{1/2}}(0) \right]. \quad (34)$$

Now we compare Eq. (34) with the matrix element of \hat{H}_{PNC} given by Eq. (4). We can write the latter in the form

$$(\hat{H}_{\text{PNC}})_{if} = \frac{\pi\alpha}{4M_Z^2} P_W \varphi_{ns_{1/2}}^+(0) \chi_{n'p_{1/2}}(0). \quad (35)$$

This comparison leads to the estimate

$$\delta_P^{\text{loop-op}} \approx \frac{1}{15\pi} \left(-\frac{Z}{N} \right) (1 - 4s^2) \alpha (\alpha Z)^2. \quad (36)$$

Now we evaluate the correction of Fig. 4b. The corresponding matrix element reads

$$S = (-i)e^2 \int d^4x_1 d^4x_2 d^4x_3 \bar{\psi}_{ns1/2}(x_1) \gamma^\mu \psi_{n'p1/2}(x_1) D_{\mu\nu}^\gamma(x_1 - x_2) \Pi_R(x_2, x_3) Z^\nu(x_3) \quad (37)$$

where $D_{\mu\nu}^\gamma(x_1 - x_2)$ is the photon propagator in Feynman gauge

$$D_{\mu\nu}^\gamma(x_1 - x_2) = \int \frac{d\omega}{2\pi} e^{-i\omega(t_1 - t_2)} D_{\mu\nu}^\gamma(\vec{x}_1 - \vec{x}_2, \omega) \quad (38)$$

with

$$D_{\mu\nu}^\gamma(\vec{x}_1 - \vec{x}_2, \omega) = -i4\pi g_{\mu\nu} \int \frac{d^3k}{(2\pi)^3} \frac{e^{i\vec{k}(\vec{x}_2 - \vec{x}_1)}}{\omega^2 - \vec{k}^2 + i\epsilon}, \quad (39)$$

and Z_ν is the external electroweak field defined by Eq. (4)

$$Z_\nu^e = \delta_{\nu 0} A_{\text{PNC}} \gamma_5 \rho_N(\vec{x}). \quad (40)$$

It turns out that the matrix element (37) is exactly zero. Returning from Fig. 4 b) to Fig. 3 b) we expand the bound electron loop in powers of the external potential (19). This expansion will contain an increasing number of Dirac matrices γ^α together with one matrix γ_5 from Eq. (40). The trace of the product of an arbitrary number of Dirac matrices can be reduced to traces of lower products. Then, using the Eqs. (26), (27) we will obtain a zero result for an arbitrary term of the bound electron loop expansion. Thus, the correction of Fig. 3 b) is absent for the nuclear spin-independent part of \hat{H}_{PNC} .

IV. LOOP CORRECTIONS TO WAVE FUNCTIONS

We start with the investigation of the graphs Fig. 4 c), d). Unlike the graphs 4 a), b) these graphs are reducible [19]. This means that the initial state of the system (the “reference” state) can be found among the intermediate states. The presence of the reference state in the sums over intermediate states leads to singularities that have to be avoided. For the solution of the “reference state” problem for the diagonal matrix element (i.e. the energy

correction) the adiabatic approach of Gell-Mann and Low [21], modified by Sucher [22] is used most frequently [19]. The extension of this approach to the nondiagonal matrix element can be most naturally formulated within the framework of the line profile QED theory [23].

Actually the graphs in Fig. 4 do not correspond to any amplitude, since the amplitude should describe some process in an atom. Still the graphs Fig. 4 a), b) are irreducible and Eq. (24) formally can be applied to them as well.

In the case of the graphs 4 c), d) we have to remember that the PNC matrix element enters necessarily in some complex amplitude describing the atomic process. In the simplest case it can be the process of photon emission by an atomic electron in one-electron ions. We will consider the situation when only two levels of opposite parity $ns_{1/2}$ and $n'p_{1/2}$ are mixed by the electroweak interaction. Actually this situation does not occur in one-electron HCl, but can be found in two-electron ions [19], [24], [25].

Instead of the graph of Fig. 4 c) we have now to consider the graph in Fig. 7 a). The corresponding S-matrix element is given by

$$S = (-i)^3 e^2 \int d^4x_1 d^4x_2 d^4x_3 \bar{\psi}_{n's_{1/2}}(x_1) \gamma^\mu A_\mu^{(\omega)*}(x_1) S_e(x_1, x_2) \gamma^\nu A_\nu^{\text{ext}}(x_2) S_e(x_2, x_3) \gamma^\lambda Z_\lambda^{(e)}(x_3) \psi_{ns_{1/2}}(x_3) , \quad (41)$$

where $A_\mu^{(\omega)*}(x)$ is the wave function of the emitted photon

$$A_\mu^{(\omega)*}(x) = \sqrt{\frac{4\pi}{2V\omega}} \vec{e}^{(\omega)*} e^{-i(\omega t - \vec{k}\vec{x})} . \quad (42)$$

\vec{e} is the polarization vector, ω , \vec{k} are the frequency and the wave vector of the photon. The external electromagnetic potential $A_\nu^{\text{ext}}(x)$ is

$$A_\nu^{\text{ext}}(x) = \delta_{\nu 0} V_U(x) , \quad (43)$$

where $V_U(x)$ is the Uehling potential [26], [27]

$$V_U(x) = \frac{2e^3 Z}{3\pi x} \int_1^\infty e^{-2mxy} \left(1 + \frac{1}{2y^2} \right) \frac{\sqrt{y^2 - 1}}{y^2} dy . \quad (44)$$

$S_e(x_1, x_2)$ denotes the electron propagator in the external field [27]

$$S_e(x_1, x_2) = \frac{1}{2\pi i} \int d\omega' e^{i\omega'(t_1-t_2)} \sum_m \frac{\psi_m(\vec{x}_1)\bar{\psi}_m(\vec{x}_2)}{E_m(1-i0) + \omega'}. \quad (45)$$

The sum over m in Eq. (45) is extended over the complete spectrum of the Dirac Hamiltonian for the electron in the field of the nucleus.

The integration over the time variables in Eq. (41) with the help of formula (24) yields

$$M_{n''s_{1/2};ns_{1/2}} = -ie^2 \sum_{m',m''} \frac{\langle n''s_{1/2}|\vec{e}\vec{A}^{(\omega)*}|m'\rangle \langle m'|V_U|m''\rangle \langle m''|H_{\text{PNC}}|ns_{1/2}\rangle}{(E_{m'} - E_{ns_{1/2}})(E_{m''} - E_{ns_{1/2}})}. \quad (46)$$

There are singular terms in the sums over m', m'' when $m', m'' = ns_{1/2}$. These singularities can be avoided by the use of the line profile theory [23]. Actually in the framework of this theory the singular terms should be omitted, but some additional terms containing derivatives of the potentials with respect to the energy can arise. In our case, due to the independence of the potentials V_U, H_{PNC} on the energy, these additional terms are absent.

Remembering now that we assumed that only one level of opposite parity $n'p_{1/2}$ is close to the initial level $ns_{1/2}$, we set $m' = n'p_{1/2}$. Then

$$M_{n''s_{1/2};ns_{1/2}} = e^2 \frac{\langle n''s_{1/2}|\vec{e}\vec{A}^{(\omega)*}|n'p_{1/2}\rangle}{E_{n'p_{1/2}} - E_{ns_{1/2}}} \sum_{m \neq ns_{1/2}} \frac{\langle n'p_{1/2}|V_U|m\rangle \langle m|H_{\text{PNC}}|ns_{1/2}\rangle}{E_m - E_{ns_{1/2}}}. \quad (47)$$

Performing the same calculations for the graph in Fig. 4d) (i.e. referring to the graph Fig. 8b)) and using the same assumptions we would obtain the expression

$$M_{n''s_{1/2};ns_{1/2}} = e^2 \frac{\langle n''s_{1/2}|\vec{e}\vec{A}^{(\omega)*}|n'p_{1/2}\rangle}{E_{n'p_{1/2}} - E_{ns_{1/2}}} \sum_{m \neq ns_{1/2}} \frac{\langle n'p_{1/2}|H_{\text{PNC}}|m\rangle \langle m|V_U|ns_{1/2}\rangle}{E_m - E_{ns_{1/2}}}. \quad (48)$$

The parts of the expressions (47) and (48) containing the sums over m yield evidently the corrections to the wave functions in the PNC matrix element. Note that we can consider the graph in Fig. 7a as a radiative loop correction to the photon emission matrix element in the parity violating photon emission amplitude.

Moreover, apart from the graphs in Fig. 7 we have, in principle, to consider also the graph in Fig. 8 which describes exclusively the radiative corrections to the photon emission. However, in this paper we will restrict ourselves only to the corrections to the PNC

matrix element. Using Eq. (41) and remembering that in the low field limit the energy denominators in Eqs. (47) and (48) are of the order $m(\alpha Z)^2$, we obtain the estimate

$$\delta_P^{\text{loop-w.f.}} \approx \alpha(\alpha Z)^2 . \quad (49)$$

Comparing (49) with the estimate (36) we conclude, that the corrections to the wave functions are dominant.

V. NUMERICAL RESULTS

In this paper we provide numerical results only for the leading loop corrections corresponding to the Feynman graphs in Fig. 4 c), d).

These leading corrections are the corrections to wave functions discussed in section 4. The loop correction corresponding to Fig. 4 a) is suppressed by the factor $(1 - 4s^2)$ in Eq. (25) and the correction corresponding to Fig. 4b is absent for the nuclear spin-independent \hat{H}_{PNC} . The electron anapole moment correction is suppressed again by the factor $(1 - 4s^2)$. The vertex corrections do not contain this suppression and should be compiled together with the loop corrections of Fig. 4 c), d). The vertex corrections will be treated separately in a subsequent paper. Thus, we retain here only the last term in Eq. (13). We performed the calculations for the PNC matrix element including the Uehling potential in the Dirac equation for the atomic electrons. This equation was solved numerically with the computer code published in [28]. Then we subtracted the same matrix element calculated without the Uehling potential. The results are listed in Table 1. The value of A_M given in the second column is: $A_M = \text{Atomic Weight}$. In the third column the nuclear radius is given. The fourth column in this Table represents the values for the PNC matrix element without the loop correction, the fifth column is the same matrix element calculated with the Uehling potential taken into account. An extended nucleus with a uniform charge distribution is employed throughout all the calculations. The nuclear radius R is taken to be

$$R = 1.2 A_M^{1/3} \text{ fm} . \quad (50)$$

In Table 2 we present the values of $\delta_P^{\text{loop-w.f.}}$ for different Z values. For $Z = 92$ this correction is 7 times smaller than main correction (11) that is insensitive to the strong field. From QED calculations we know, that the vacuum polarization corrections are strongly sensitive to the field, i.e., results obtained in the low field approximation and extrapolated to the strong field case differ from the accurate strong field calculation by 100% and more. From Tables 1, 2 we can deduce, that the strong field effect for the electroweak radiative corrections in HCI exceeds 10% for $Z = 92$. This is an order of magnitude higher than could be expected from the simple extrapolation of the Lynn and Sandars [6] values. The results obtained here demonstrate that the experiments with HCI would provide the possibility to test the Standard Model in the strong field. The most likely candidate for future PNC experiments with HCI is the He-like uranium ion [24], [25], [29]. The theory developed in the present paper allows for the evaluation of all the electroweak radiative corrections for this ion as well.

VI. ACKNOWLEDGMENTS

The authors are grateful to Dr. M. G. Kozlov for fruitful discussions. The work of I. B. and L. L. was supported by the Russian Fund for Fundamental Investigations, grant $N \overset{0}{=} 99 - 02 - 18526$, the work of I. B. also by the Administration of St. Petersburg, grant $N \overset{0}{=} M - 97 - 2.2d - 974$. G.S. acknowledges support by the BMBF, the DFG, and by GSI (Darmstadt).

TABLES

Z	A_M	R_{nucl}	PNC	PNC(Uehl.)
1	1.007	1.212	.1954019E-17	.1954049E-17
2	4.001	1.921	-.7939763E-15	-.7940027E-15
3	6.939	2.307	-.8095202E-14	-.8095641E-14
4	9.010	2.517	-.3254761E-13	-.3255015E-13
5	10.807	2.675	-.9200810E-13	-.9201771E-13
6	12.007	2.770	-.1960428E-12	-.1960690E-12
7	14.002	2.916	-.4258223E-12	-.4258927E-12
8	15.995	3.048	-.8348039E-12	-.8349702E-12
9	18.994	3.228	-.1698600E-11	-.1698998E-11
10	20.173	3.293	-.2637995E-11	-.2638717E-11
20	40.069	4.140	-.9367160E-10	-.9374468E-10
30	65.363	4.874	-.1014421E-08	-.1015930E-08
40	91.198	5.446	-.5932577E-08	-.5946879E-08
50	118.662	5.945	-.2623394E-07	-.2632746E-08
60	144.207	6.345	-.9515140E-07	-.9562729E-07
70	173.001	6.742	-.3259331E-06	-.3281342E-06
80	200.546	7.082	-.1044648E-05	-.1053974E-05
82	207.155	7.159	-.1325790E-05	-.1338273E-05
90	231.989	7.434	-.3371690E-05	-.3410852E-05
92	234.993	7.466	-.4167152E-05	-.4218238E-05
92	238.000	7.498	-.4249630E-05	-.4301619E-05

TABLE I. Loop correction to the wave functions in the PNC matrix element for $n = n' = 2$. The values of the matrix elements are given in eV. The nuclear radius is given in units of fm.

Z	A_M	R_{nucl}	$\delta_{\text{P}}^{\text{loopw.f.}}$
1	1.007	1.212	.1528E-04
2	4.001	1.921	.3332E-04
3	6.939	2.307	.5414E-04
4	9.010	2.517	.7790E-04
5	10.807	2.675	.1044E-03
6	12.007	2.770	.1339E-03
7	14.002	2.916	.1653E-03
8	15.995	3.048	.1992E-03
9	18.994	3.228	.2343E-03
10	20.173	3.293	.2736E-03
20	40.069	4.140	.7801E-03
30	65.363	4.874	.1488E-02
40	91.198	5.446	.2410E-02
50	118.662	5.945	.3564E-02
60	144.207	6.345	.5001E-02
70	173.001	6.742	.6753E-02
80	200.546	7.082	.8927E-02
82	207.155	7.159	.9415E-02
90	231.989	7.434	.1161E-01
92	234.993	7.466	.1223E-01
92	238.000	7.498	.1225E-01

TABLE II. The wave function contribution to Δ_{rad} (Eq. (13)).

REFERENCES

- [1] Review of Particle Properties, Particle Physics Booklet, AIP, July 1996
- [2] M. S. Peskin and T. Takeuchi, Phys. Rev. D46, 381 (1992)
- [3] A. Sirlin, Phys. Rev. D22, 971 (1980)
- [4] W. J. Marchiano and J. L. Rosner, Phys. Rev. Lett. 65, 2963 (1990)
- [5] K. T. Mahanthappa and P. K. Mohapatra, Phys. Rev D43, 3093 (1991)
- [6] B. W. Lynn and P. G. H. Sandars, J. Phys. B27, 1469 (1994)
- [7] M. A. Bouchiat and C. C. Bouchiat, Phys. Lett. 48b, 111 (1974)
- [8] J. Schweppe, A. Belkacem, L. Blumenfeld, N. Claytor, B. Feinberg, H. Gould, V. E. Kloster, L. Levy, S. Misawa, J. R. Mowat, M. H. Prior, Phys. Rev. Lett. 66, 1434 (1989)
- [9] Th. Stöhlker, P. H. Mokler, K. Beckert, F. Bosch, H. Eickhoff, B. Franzke, M. Jung, T. Kandler, O. Kleppner, C. Kuzuharov, R. Moshhammer, F. Nolden, H. Reich, P. Rymuza, P. Spädtker, M. Steck, Phys. Rev. Lett. 71, 2184 (1993)
- [10] H. F. Beyer, G. Menzel, D. Liesen, A. Gallus, F. Bosch, R. D. Deslattes, P. Indelicato, Th. Stöhlker, O. Kleppner, R. Moshhammer, F. Nolden, H. Eickhoff, B. Franzke, M. Steck, Z. Phys. D35, 169 (1995)
- [11] H. F. Beyer, D. Liesen, F. Bosch, K. D. Finlayson, M. Jung, O. Kleppner, R. Moshhammer, K. Beckert, H. Eickhoff, B. Franzke, F. Nolden, P. Spädtker, M. Steck, G. Menzel, R. D. Deslattes, Phys. Lett. A184, 435 (1994)
- [12] Th. Beier and G. Soff, Z. Phys. D8, 129 (1988)
- [13] S. M. Schneider, W. Greiner and G. Soff, J. Phys. B26, L529 (1993)
- [14] I. Lindgren, H. Persson, S. Salomonson, V. Karasiev, L. Labzowsky, A. Mitruschenkov and M. Tokman, J. Phys. B26, L503 (1993)

- [15] A. Mitrushenkov, L. Labzowsky, I. Lindgren, H. Persson and S. Salomonson, Phys. Lett. A200, 51 (1995)
- [16] H. Persson, I. Lindgren, L. Labzowsky, G. Plunien, T. Beier and G. Soff, Phys. Rev. A54, 2805 (1996)
- [17] S. Mallampalli and J. Sapirstein, Phys. Rev. A54, 2714 (1996)
- [18] P. G. H. Sandars, J. Phys. B23, L655 (1990)
- [19] L. Labzowsky, G. Klimchitskaya and Yu. Dmitriev, *Relativistic Effects in Atomic System*, (IOP, Bristol and Philadelphia, 1993)
- [20] N. N. Bogolyubov and D. V. Shirkov, *Quantenfelder*, (Physik-Verlag, Weinheim, 1985)
- [21] M. Gell-Mann and F. Low, Phys. Rev. 84, 350 (1951)
- [22] J. Sucher, Phys. Rev. 107, 1448 (1957)
- [23] L. Labzowsky, V. Karasiev, I. Lindgren, H. Persson and S. Salomonson, Phys. Scripta T46, 150 (1993)
- [24] A. Schäfer, G. Soff, P. Indelicato, B. Müller and W. Greiner, Phys. Rev. A40, 7362 (1989)
- [25] V. V. Karasiev, L. N. Labzowsky and A. V. Nefiodov, Phys. Lett. A172, 62 (1995)
- [26] E. A. Uehling, Phys. Rev. 48, 55 (1935)
- [27] A. Akhiezer and V. Berestetskii, *Quantum Electrodynamics*, (Wiley, New York, 1965)
- [28] F. Salvat and R. Mayol, Comput. Phys. Commun. 62, 65 (1991)
- [29] R. W. Dunford, Phys. Rev. A54, 3820 (1996)

FIGURES

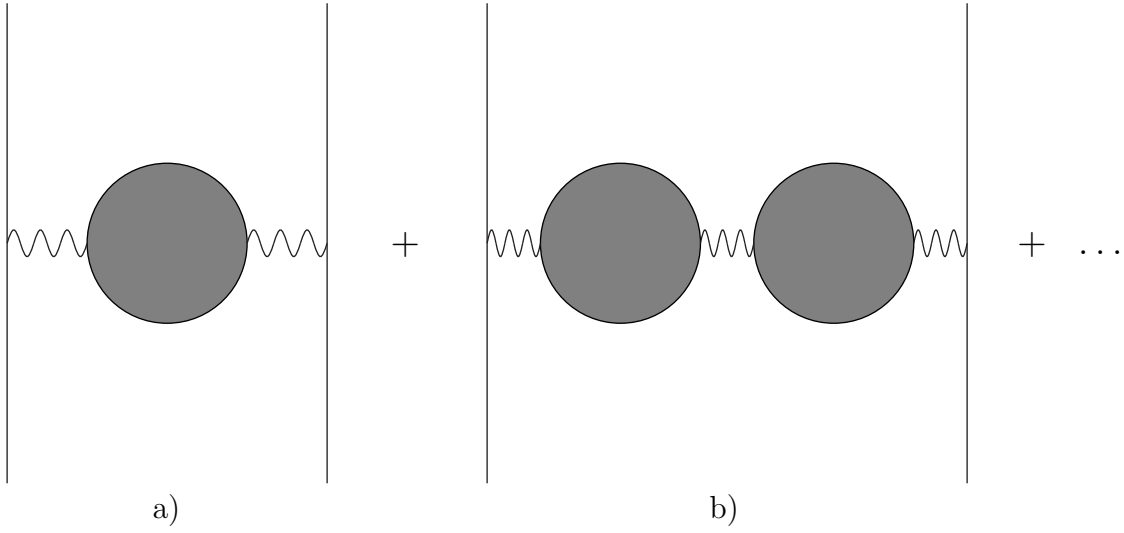


FIG. 1. The Feynman graphs corresponding to the “oblique” corrections. The solid line correspond to fermions, the wavy line correspond to vectors (W^+, W^-, Z, γ), the dark circles denote the fermion, vector and scalar loops.

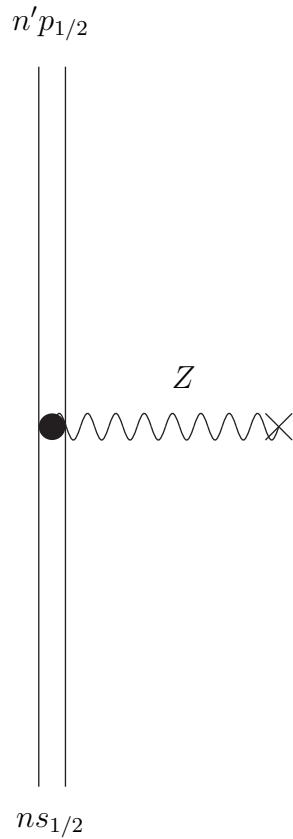


FIG. 2. The Feynman graph corresponding to the basic atomic matrix element in the Furry picture. The double solid line denotes the electron in the field of the nucleus. The wavy Z line with the cross at the end denotes the interaction with the field given by Eq. (4).

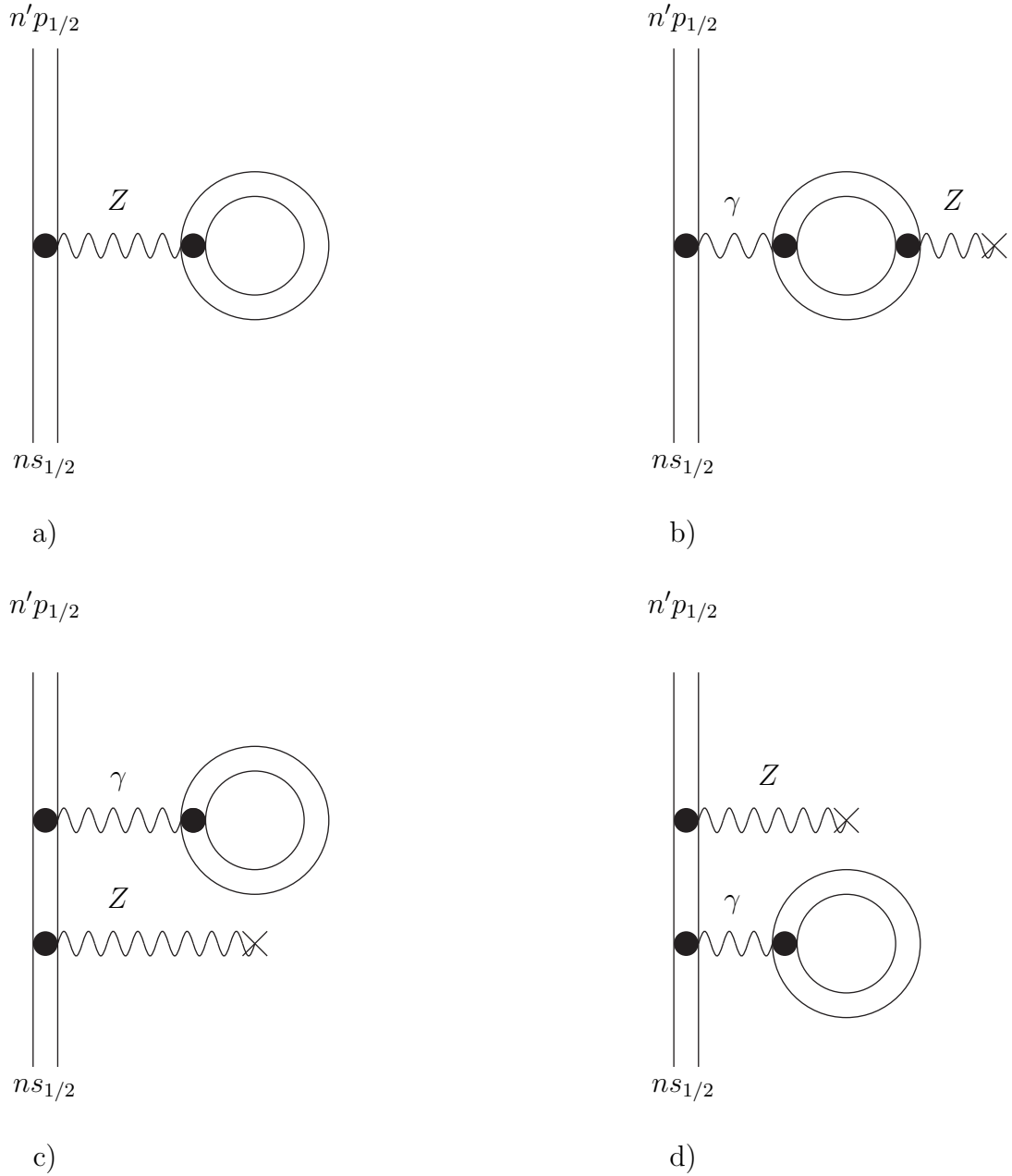
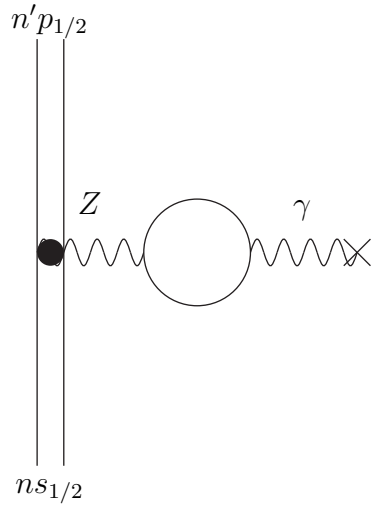
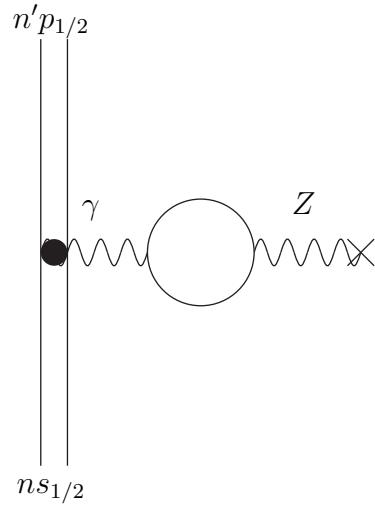


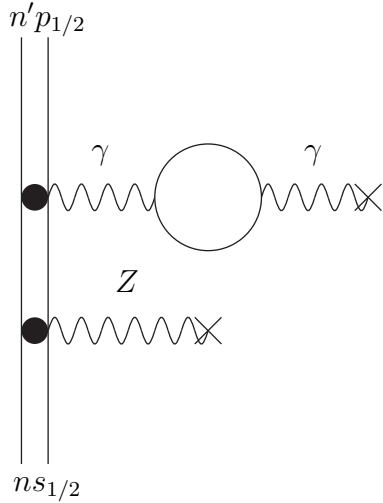
FIG. 3. The Feynman graphs with electron loops contributing to the electroweak radiative corrections. Notations are the same as in Fig. 2. The wavy Z line denotes the Z -boson, the wavy γ line denotes the photon.



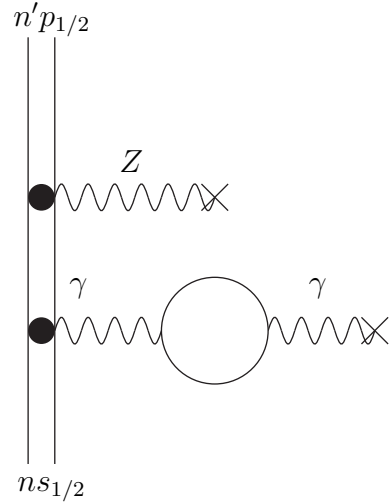
a)



b)



c)



d)

FIG. 4. The Feynman graphs corresponding to the loop corrections in the Uehling approximation. The wavy γ line with the cross at the end denotes the electromagnetic interaction with the nucleus.

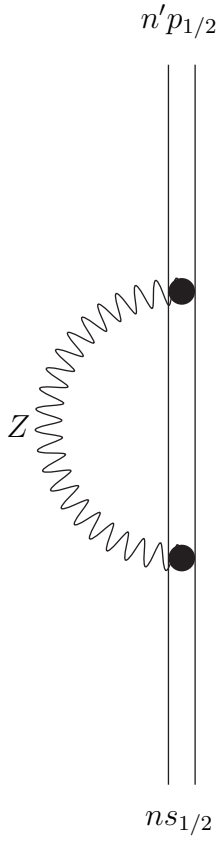


FIG. 5. The Feynman graph that represents the electron anapole moment correction to the basic atomic PNC matrix element in the Furry picture. Notations are the same as in Fig. 2.

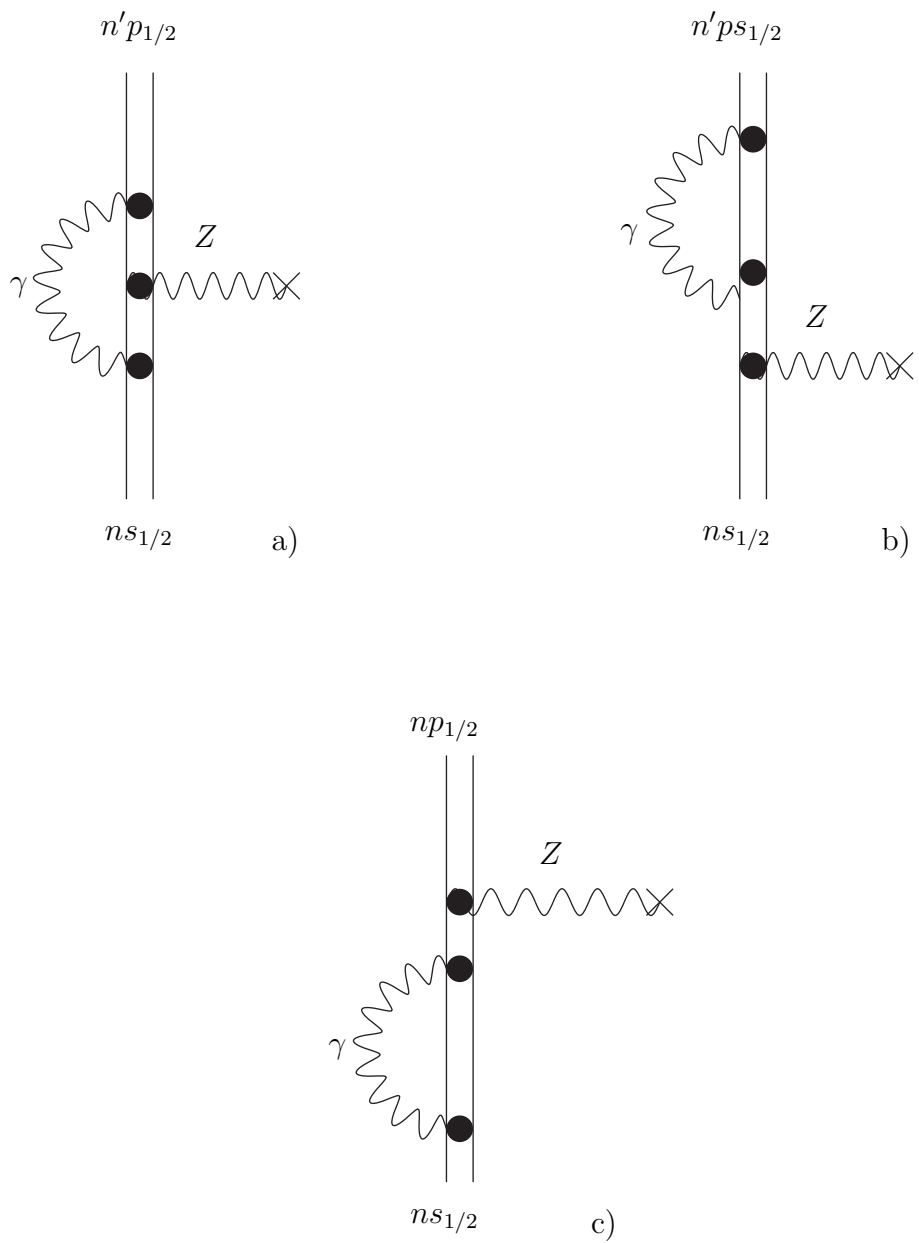


FIG. 6. Feynman graphs that represent the corrections caused by the electromagnetic renormalization of the Z coupling.

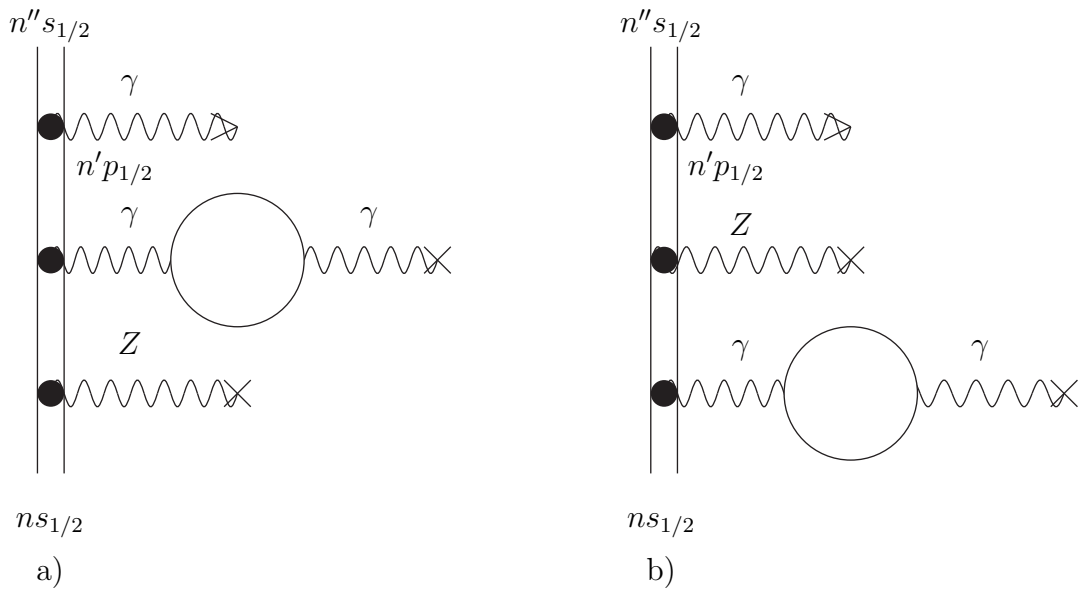


FIG. 7. Feynman graphs for the amplitude of the process of the photon emission including PNC.

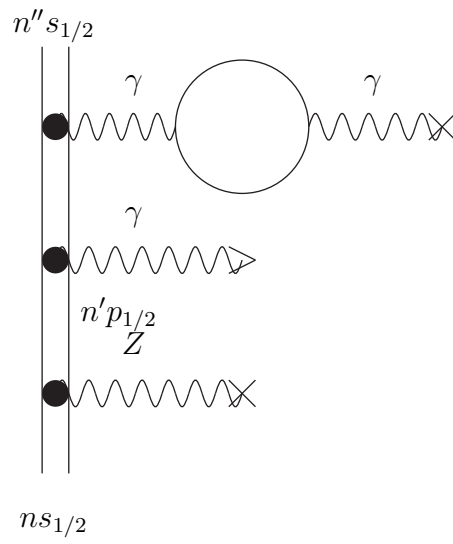


FIG. 8. Feynman graph that describes the radiative corrections to the emission matrix element.